Supplementary Materials, Fig.S1

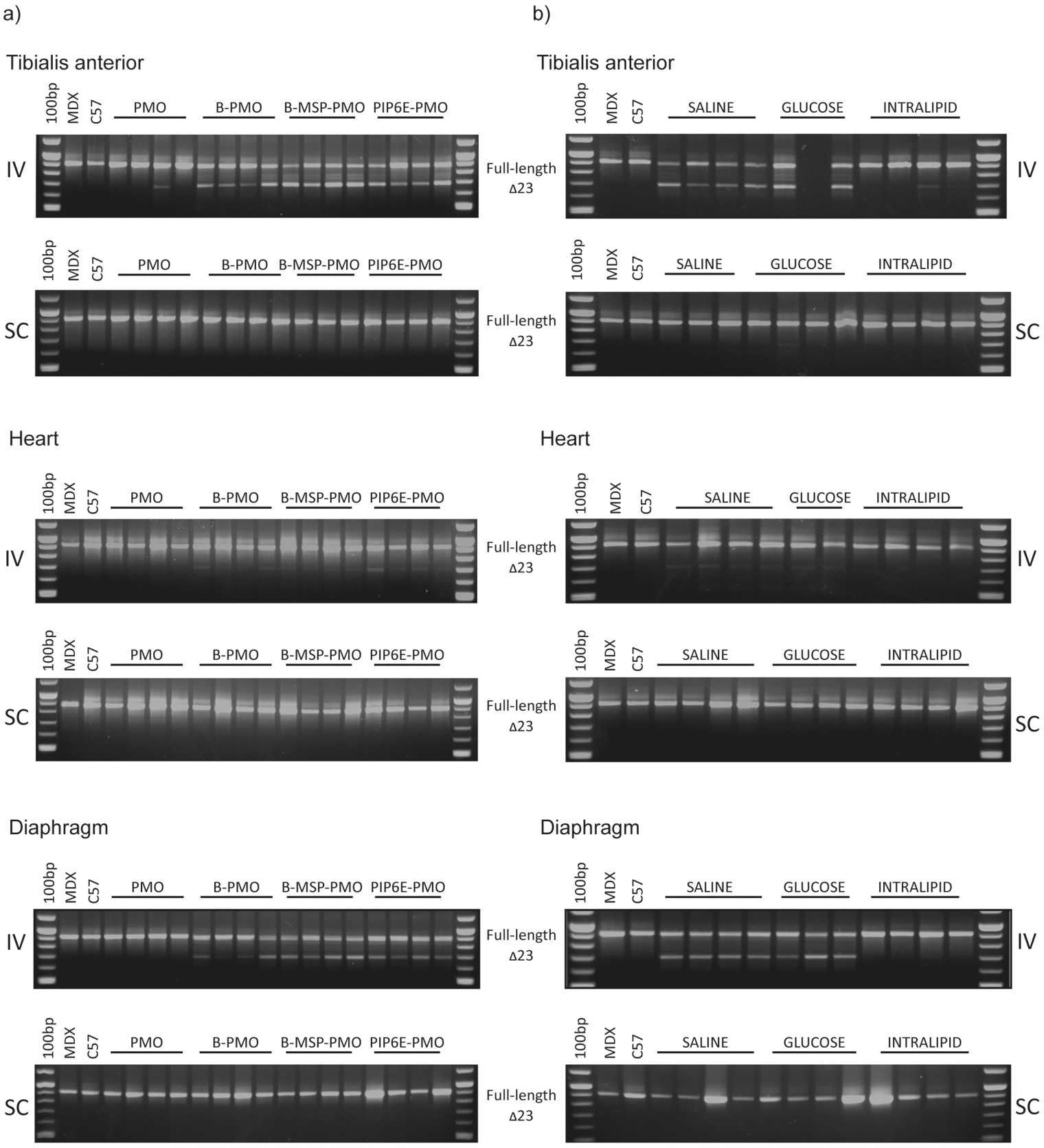

Supplementary Materials, Fig. S1. **Exon skipping analysis following P-PMO route and formulation studies.** In order to develop the optimal delivery of P-PMO, we investigated whether routes of administration or alternative formulation of P-PMO prior to injection, could influence their efficacy. (**A**) Intravenous and subcutaneous injection of three different peptide conjugates was performed (B-PMO, B-MSP-PMO and Pip6e-PMO) and their activities were compared to naked PMO. (**B**) Pip6e-PMO was formulated in either 5% D-glucose, physiological saline or intralipid prior to injection via the tail vein. Male *mdx* mice (n=4) received a dose of 12.5mg/kg. Tissues were harvested 2 weeks post-injection. Exon skipping levels were assessed two weeks post injection. Nested PCR was performed on 400ng RNA from TA, heart and diaphragm, with skipping of exon 23 indicated by the presence of a band at 688bp compared to the full length band at 901bp. PMO; phosphorodiamidate morpholino oligonucleotide.

Supplementary Materials, Fig. S2

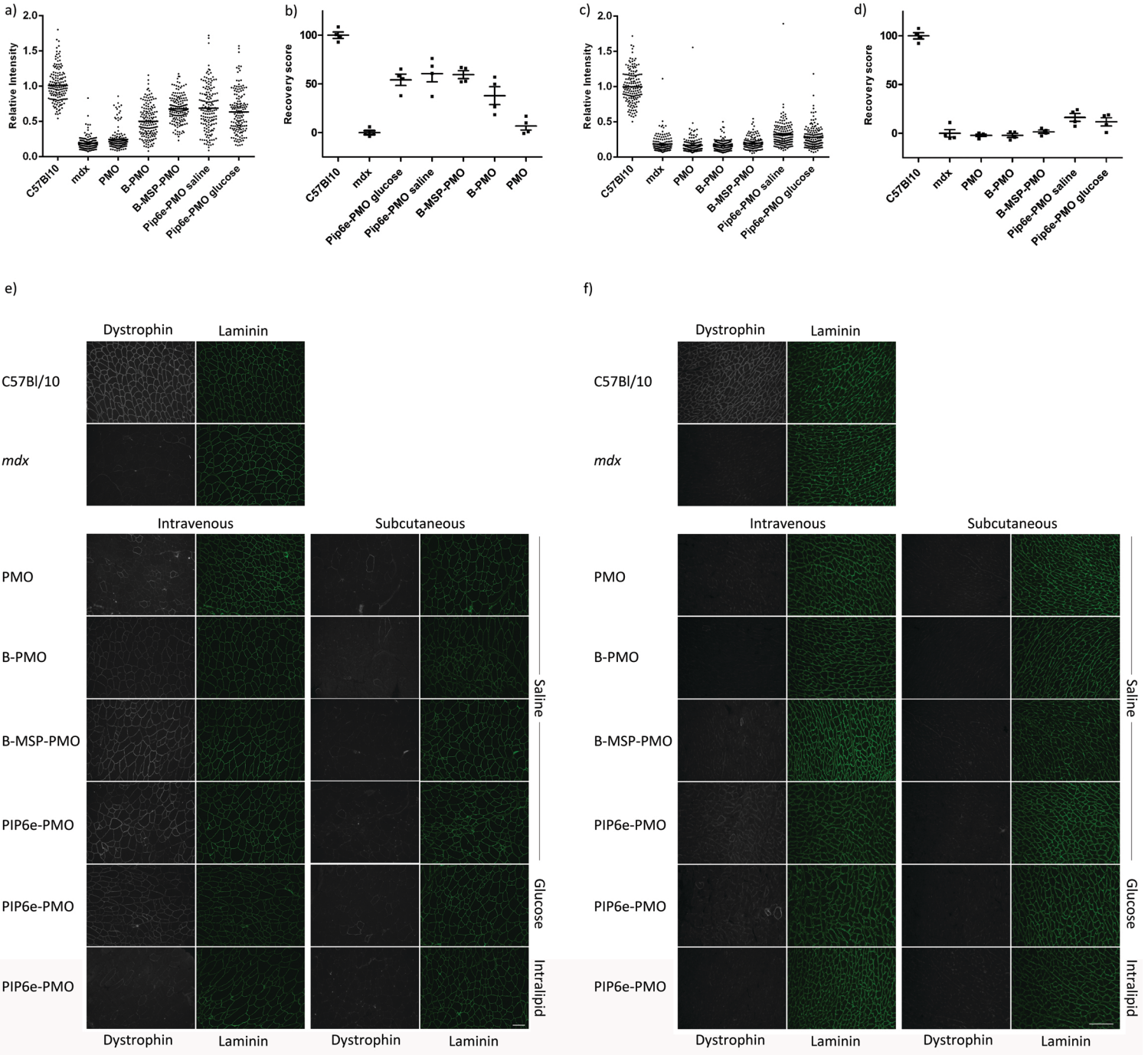

Supplementary Materials, Fig. S2. **Sarcolemmal dystrophin restoration analysis following P-PMO route and formulation studies.** In order to develop the optimal delivery of PPMO, we investigated whether routes of administration or alternative formulation of P-PMO prior to injection, could influence their efficacy. Intravenous and subcutaneous injection of three different peptide conjugates was performed (B-PMO, B-MSP-PMO and Pip6e-PMO) and their activities were compared to naked PMO. Pip6e-PMO was formulated in either 5% D-glucose, physiological saline or intralipid prior to injection via the tail vein. Male *mdx* mice (n=4) received a dose of 12.5mg/kg. Tissues were harvested 2 weeks post-injection. Sarcolemmal-associated dystrophin expression was assessed by immunostaining. Sarcolemmal intensity measurements quantified dystrophin relative to laminin-α2 and normalised to C57Bl/10 in the TA (**A**) and heart (**C**). Mean intensity values were used to generate a percentage recovery score (0%; untreated *mdx*, 100%; C57Bl/10) in the TA (**B)** and heart (**D**). Error bars represent SEM. Representative images of dystrophin staining in the TA and heart two weeks post injection are shown in (**E**) and (**F**) respectively. Scale bar, 100 microns. Wks; weeks. PMO; phosphorodiamidate morpholino oligonucleotide.

Supplementary Materials, Fig.S3

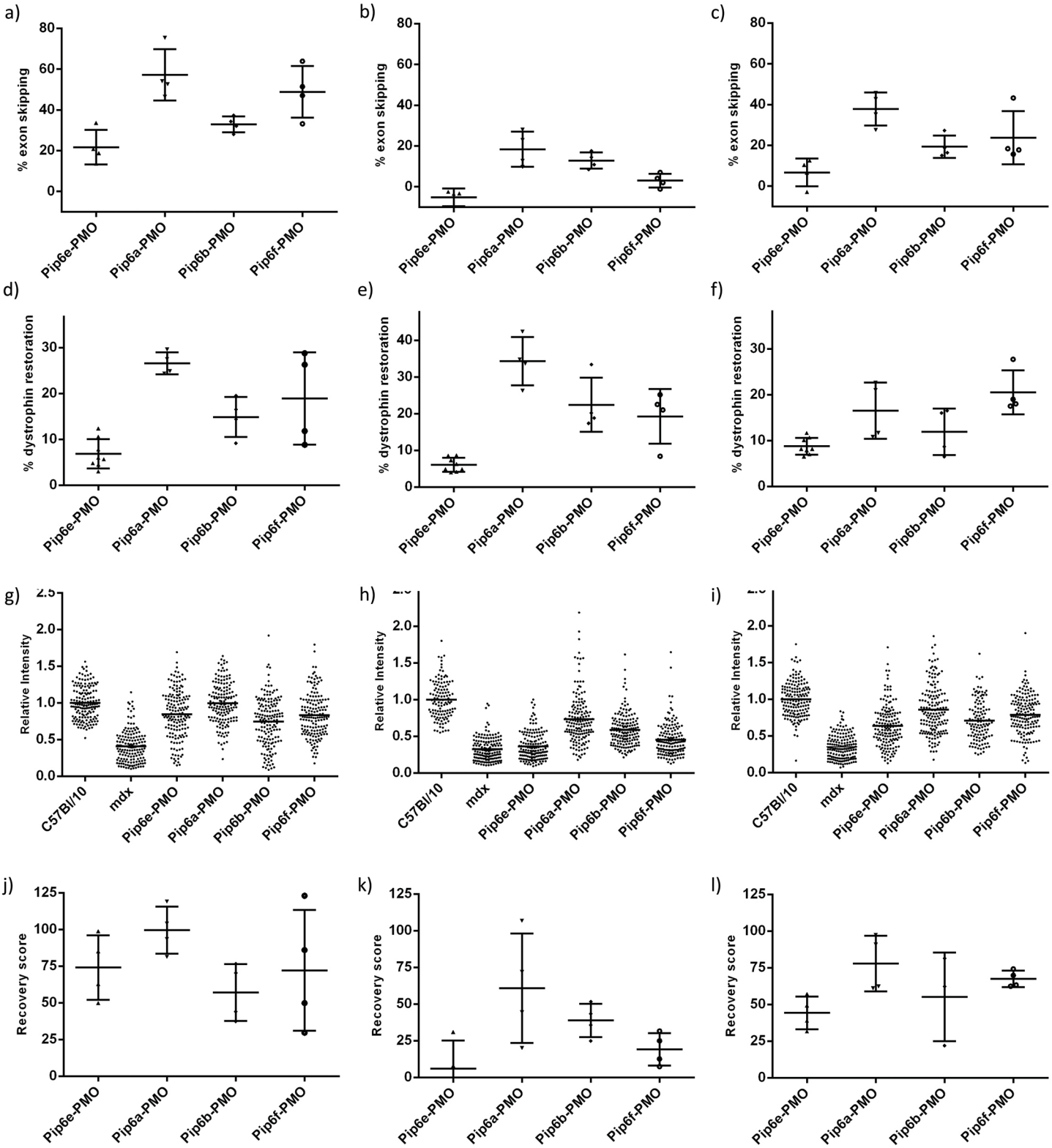

Supplementary Materials, Fig. S3. **Pip6-peptide comparison study.** Twelve-week old male *mdx* mice were treated with a single 12.5mg/kg intravenous dose of either Pip6e-PMO, Pip6a-PMO, Pip6b-PMO or Pip6f-PMO formulated in physiological saline. Tissues were harvested 2 weeks post-injection. RT-qPCR was performed to determine *Dmd* exon 23 exclusion in the TA **(A)**, heart **(B)** and diaphragm **(C)**. Total dystrophin protein restoration was assessed by western blot using an infrared detection system in the TA **(D)**, heart **(E)** and diaphragm **(F)**. Sarcolemmal-associated dystrophin expression was assessed by immunostaining. Sarcolemmal intensity measurements quantified dystrophin relative to laminin-α2 and normalised to C57Bl/10 in the TA **(G)**, heart **(H)** and diaphragm **(I)**. (**J**-**L**) Mean intensity values were used to generate a percentage recovery score (0%; untreated *mdx*, 100%; C57Bl/10). Error bars represent SEM. PMO; phosphorodiamidate morpholino oligonucleotide.

Supplementary Materials, Fig.S4

a)

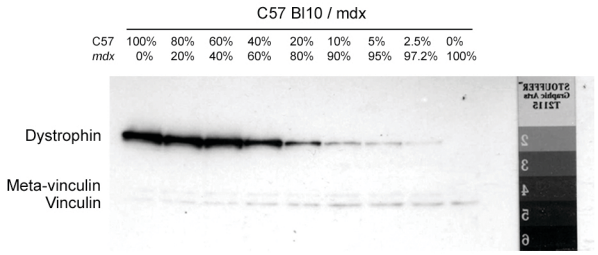

b)

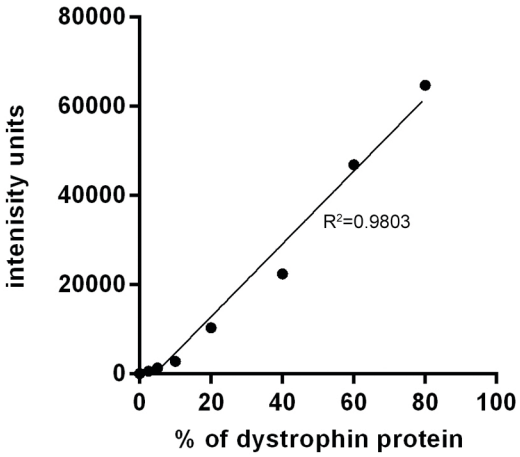

Supplementary Materials, Fig. S4. **Linear range analysis for western blot. (A)** Standard curve generated by mixing different percentages of C57Bl/10 and *mdx* muscle samples to maintain an equal protein load in each track with varying dystrophin levels. Vinculin was used as an internal loading control. An optical density control strip (Stouffer industries, inc.) is shown on the right of the image and was scanned simultaneously. (**B)** The relationship between intensity units and dystrophin (corrected for loading using vinculin) was linear between 2.5% and 80% (R^2=0.98). PMO; phosphorodiamidate morpholino oligonucleotide.

Supplementary Materials, Fig.S5

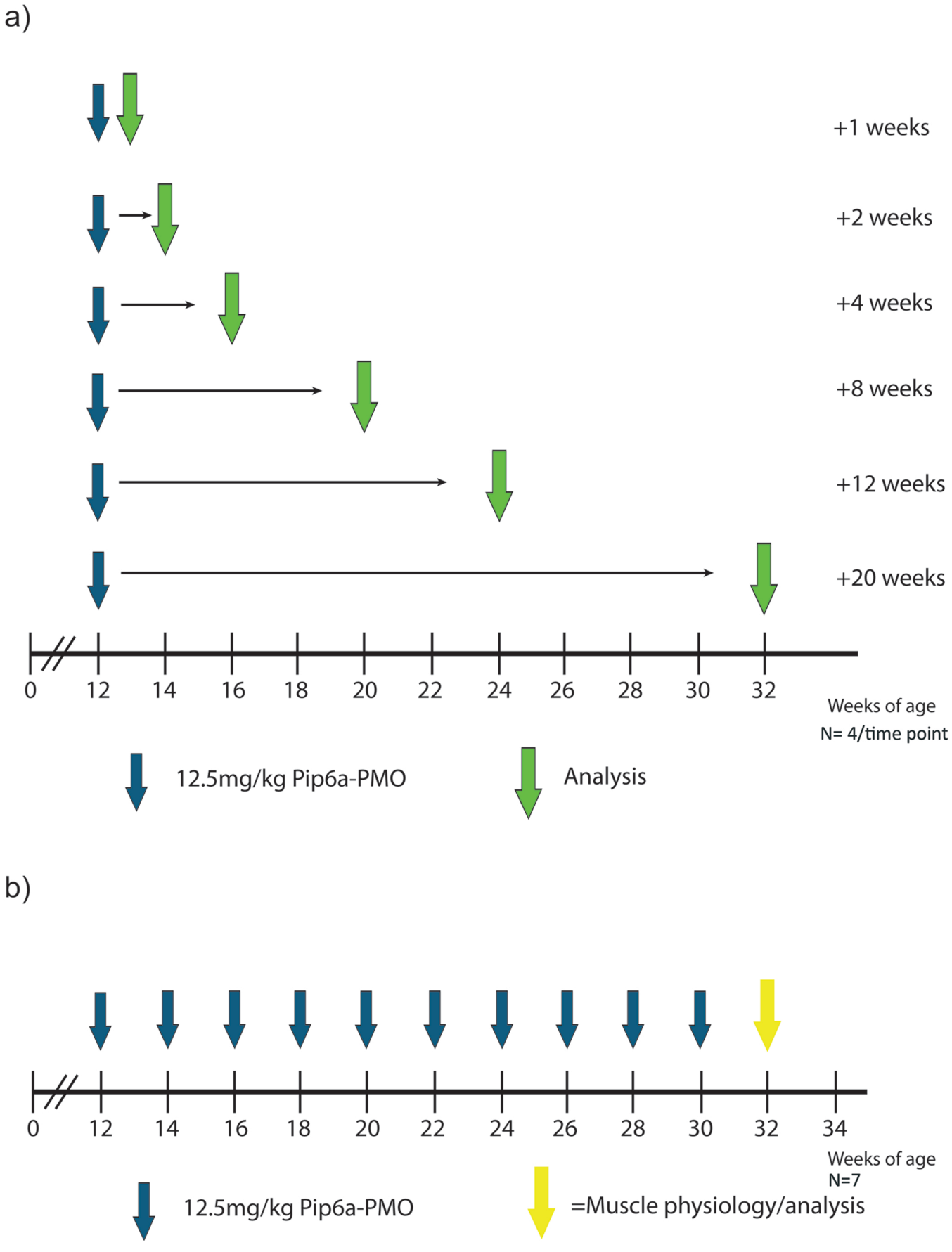

Supplementary Materials, Fig. S5. **Schematics of experimental design.** Regimens used to evaluate the duration of AO induced exon skipping and dystrophin restoration (**A**) and the functional consequences of chronic Pip6a-PMO administration (**B**). Blue arrows represent systemic P-PMO administration. Tissue harvests are represented by green arrows. Yellow arrow represents muscle physiology analysis. PMO; phosphorodiamidate morpholino oligonucleotide.

Supplementary Materials, Fig. S6

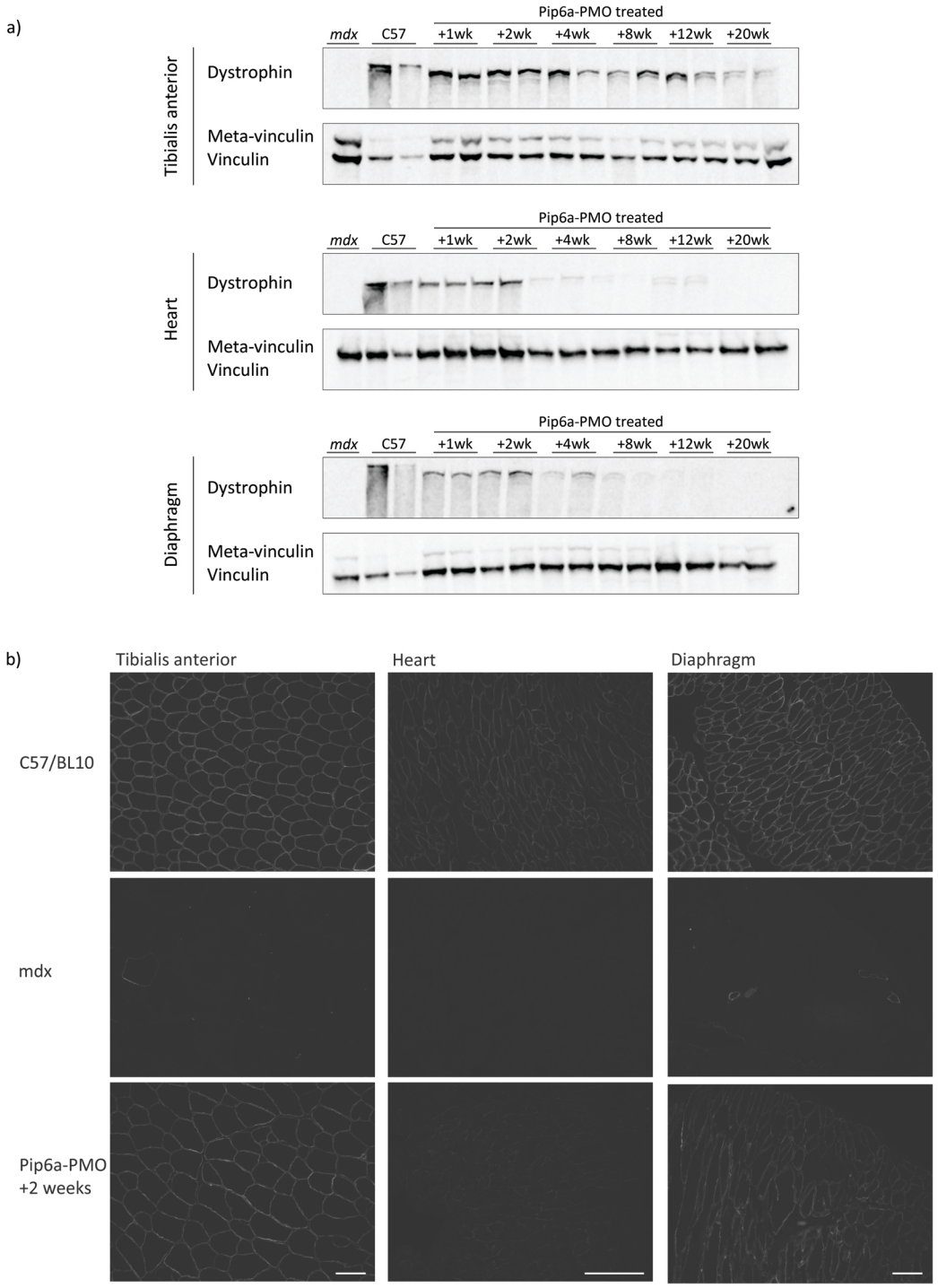

Supplementary Materials, Fig. S6. **The duration of dystrophin restoration following Pip6a-PMO administration.** Twelve-week old male *mdx* mice were treated with a single 12.5mg/kg intravenous dose of Pip6a-PMO. Tissues were harvested 1, 2, 4, 8, 12 and 20 weeks post-injection. **(A)** Total dystrophin protein restoration was assessed by western blot using an infrared detection system. Due to the variable expression of meta-vinculin between tissues, dystrophin levels are reported relative to vinculin levels. Representative images of membranes are shown. **(B)**Sarcolemmal-associated dystrophin expression was assessed by immunostaining. Representative images of dystrophin staining 2 weeks post injection are shown in. Scale bar, 100 microns. Wks; weeks. PMO; phosphorodiamidate morpholino oligonucleotide.

Supplementary Materials, Fig. S7

a)

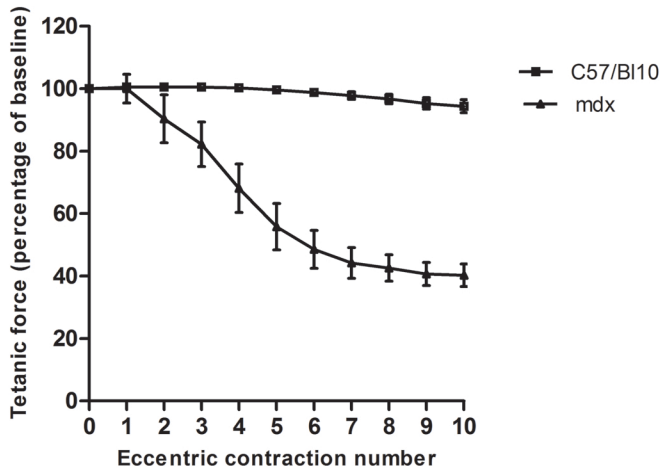

b)

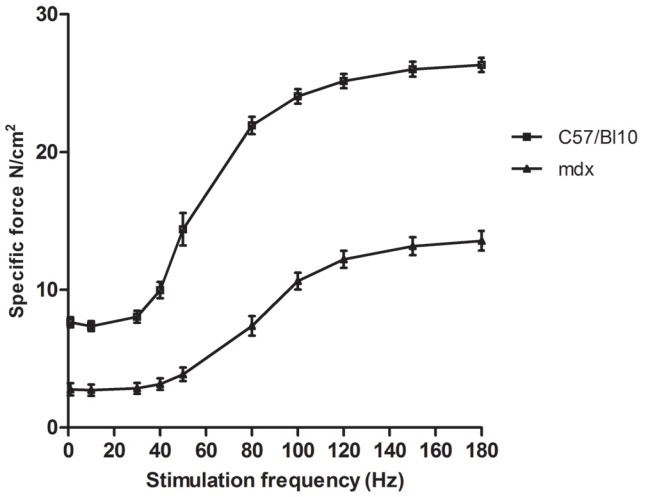

Supplementary Materials, Fig. S7. **Physiological parameters in C57Bl/10 and *mdx* mice.** **(A)** Graph showing the difference in resistance to eccentric contraction-induced muscle damage during an *in situ* exercise protocol in 32-week old C57Bl/10 male mice and age/sex matched *mdx* mice. **(B)** Force-frequency curve comparing tetanic force production at different stimulations (1-180Hz) in 32-week old C57Bl/10 male mice and age/sex matched *mdx* mice. N=7. Error bars represents SEM.

Supplementary Materials, Fig.S8

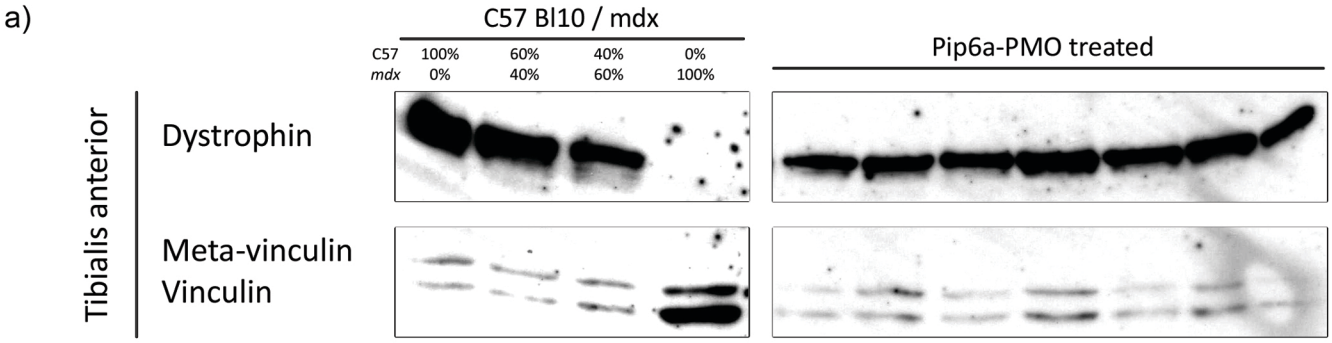

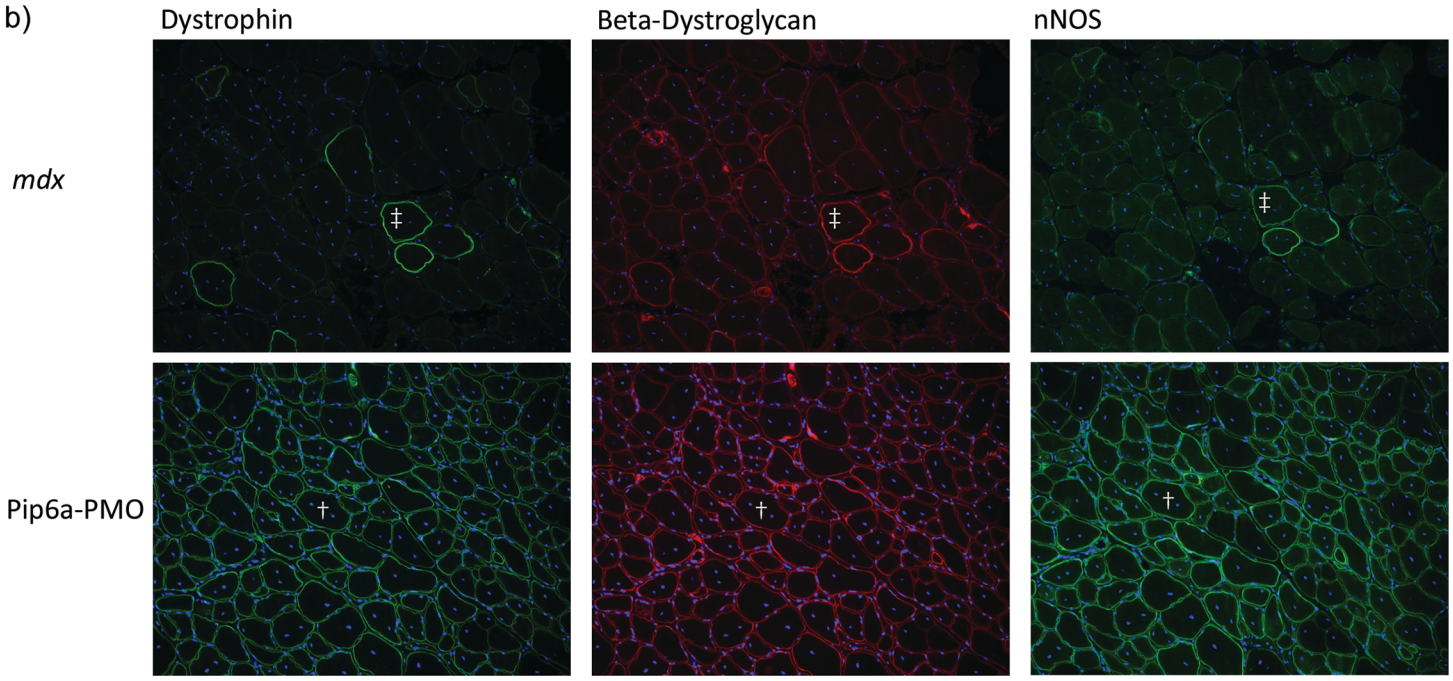

Supplementary Materials, Fig. S8. **Dystrophin and DAPC restoration after chronic delivery of Pip6a-PMO. (A)** Western blot analysis of total dystrophin protein 2 weeks after the last systemic Pip6a-PMO injection. A standard curve was generated by mixing C57Bl/10 and *mdx* muscle samples; this maintains equal amounts of the loading of protein, vinculin, throughout the standard curve. Additional *mdx* total protein was loaded into lane 4 to demonstrate the absence of dystrophin staining in untreated mice. On average, 50% of internally deleted dystrophin expression levels (relative to wild-type) were restored in TA muscles of Pip6a-PMO treated *mdx* mice. Western blot gels were run at the same time. (**B)** Representative images showing homogenous dystrophin expression co-localising with beta-dystroglycan and neuronal nitric oxide synthase (nNOS) in the TA. Dystrophin, beta-dystroglycan and nNOS expression was noted in revertant myofibres in littermate control *mdx* mice. White crosses $^{(\dagger,\ddagger)}$ represent the same myofibre in serial TA muscle cryosections. Scale bar, 100 microns. PMO; phosphorodiamidate morpholino oligonucleotide; TA; tibialis anterior.

Supplementary Materials, Fig.S9

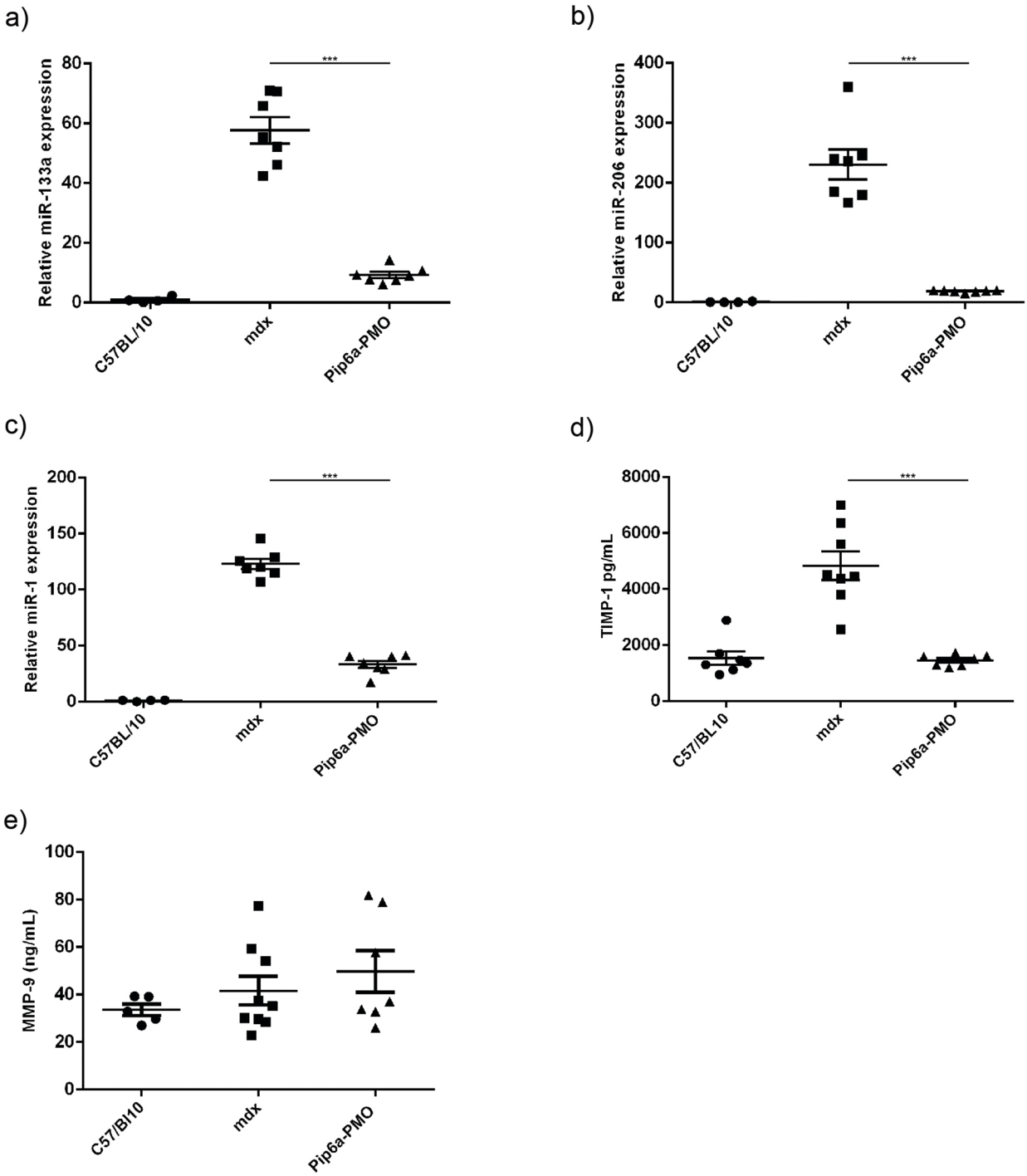

Supplementary Materials, Fig. S9. **Partial and complete normalisation of serum biomarkers in Pip6a-PMO treated mice.** Analysis of circulating miRNAs showed partial or complete normalisation to C57Bl/10 wild-type mice levels in miR133a (**A**), miR-206 (**B**) and miR-1 (**C**). **(D)** In addition, serum TIMP-1 levels were restored to wild-type levels (1542.4±241.9 pg/mL) in Pip6a-PMO treated mice (1456.9±77.61 pg/mL), in contrast to untreated littermate control mice (4831±504.6 pg/mL). **(E)** No significant difference in MMP-9 was noted between treated, non-treated *mdx* mice and aged match C57Bl/10 mice. PMO, phosphorodiamidate morpholino oligonucleotide. Kruskal-Wallis analysis with Dunn's *post hoc* test, *** p=<0.001, n=7.